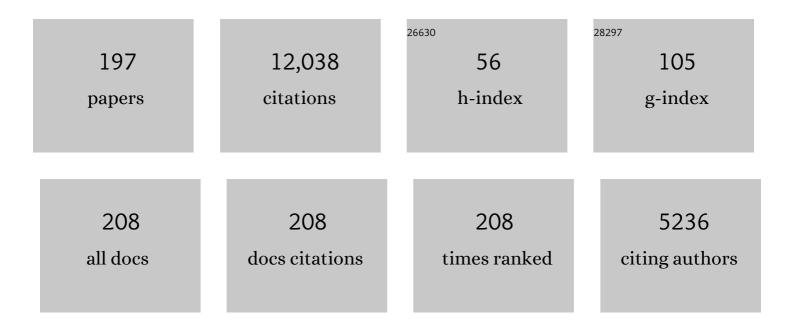
Fabrizio Capaccioni

List of Publications by Year in descending order

Source: https://exaly.com/author-pdf/7961952/publications.pdf Version: 2024-02-01



FARRIZIO CARACCIONI

#	Article	IF	CITATIONS
1	AMBITION – comet nucleus cryogenic sample return. Experimental Astronomy, 2022, 54, 1077-1128.	3.7	4
2	Saturn's icy satellites investigated by Cassini - VIMS. V. Spectrophotometry. Icarus, 2022, 375, 114803.	2.5	3
3	Spectral Units Analysis of Quadrangle H05â€Hokusai on Mercury. Journal of Geophysical Research E: Planets, 2022, 127, .	3.6	7
4	Water ortho-to-para ratio in the coma of comet 67P/Churyumov-Gerasimenko. Astronomy and Astrophysics, 2022, 663, A43.	5.1	3
5	Macro and micro structures of pebble-made cometary nuclei reconciled by seasonal evolution. Nature Astronomy, 2022, 6, 546-553.	10.1	20
6	Optical performance evaluation of the high spatial resolution imaging camera of BepiColombo space mission. Optics and Laser Technology, 2021, 141, 107172.	4.6	4
7	Laboratory characterization of HYPSOS, a novel 4D remote sensing instrument. , 2021, , .		1
8	The surface distributions of the production of the major volatile species, H2O, CO2, CO and O2, from the nucleus of comet 67P/Churyumov-Gerasimenko throughout the Rosetta Mission as measured by the ROSINA double focusing mass spectrometer. Icarus, 2020, 335, 113421.	2.5	57
9	The Philae lander reveals low-strength primitive ice inside cometary boulders. Nature, 2020, 586, 697-701.	27.8	40
10	Photometric modelling and VIS-IR albedo maps of Rhea from Cassini-VIMS. Monthly Notices of the Royal Astronomical Society: Letters, 2020, 499, L62-L66.	3.3	3
11	Temporal evolution of the permanent shadowed regions at Mercury poles: applications for spectral detection of ices by SIMBIOSYS-VIHI on BepiColombo mission. Monthly Notices of the Royal Astronomical Society, 2020, 498, 1308-1318.	4.4	3
12	Ammonium salts are a reservoir of nitrogen on a cometary nucleus and possibly on some asteroids. Science, 2020, 367, .	12.6	115
13	SIMBIO-SYS: Scientific Cameras and Spectrometer for the BepiColombo Mission. Space Science Reviews, 2020, 216, 1.	8.1	47
14	Rationale for BepiColombo Studies of Mercury's Surface and Composition. Space Science Reviews, 2020, 216, 1.	8.1	46
15	Infrared detection of aliphatic organics on a cometary nucleus. Nature Astronomy, 2020, 4, 500-505.	10.1	41
16	Development of a simulator of the SIMBIOSYS suite onboard the BepiColombo mission. Monthly Notices of the Royal Astronomical Society, 2020, 491, 1673-1689.	4.4	1
17	An orbital water-ice cycle on comet 67P from colour changes. Nature, 2020, 578, 49-52.	27.8	36
18	Hydroxylated Mg-rich Amorphous Silicates: A New Component of the 3.2 μm Absorption Band of Comet 67P/Churyumov–Gerasimenko. Astrophysical Journal Letters, 2020, 897, L37.	8.3	12

#	Article	IF	CITATIONS
19	Cassini-VIMS observations of Saturn's main rings: II. A spectrophotometric study by means of Monte Carlo ray-tracing and Hapke's theory. Icarus, 2019, 317, 242-265.	2.5	17
20	Global Spectral Properties and Lithology of Mercury: The Example of the Shakespeare (Hâ€03) Quadrangle. Journal of Geophysical Research E: Planets, 2019, 124, 2326-2346.	3.6	10
21	Analysis of night-side dust activity on comet 67P observed by VIRTIS-M: a new method to constrain the thermal inertia on the surface. Astronomy and Astrophysics, 2019, 630, A21.	5.1	8
22	The changing temperature of the nucleus of comet 67P induced by morphological and seasonal effects. Nature Astronomy, 2019, 3, 649-658.	10.1	34
23	Visible and Near-Infrared Spectral Analyses of Asteroids and Comets from Dawn and Rosetta. , 2019, , 413-427.		0
24	Synthesis of the morphological description of cometary dust at comet 67P/Churyumov-Gerasimenko. Astronomy and Astrophysics, 2019, 630, A24.	5.1	100
25	VIRTIS-H observations of the dust coma of comet 67P/Churyumov-Gerasimenko: spectral properties and color temperature variability with phase and elevation. Astronomy and Astrophysics, 2019, 630, A22.	5.1	17
26	Diurnal variation of dust and gas production in comet 67P/Churyumov-Gerasimenko at the inbound equinox as seen by OSIRIS and VIRTIS-M on board Rosetta. Astronomy and Astrophysics, 2019, 630, A23.	5.1	9
27	NIR reflectance spectroscopy of hydrated and anhydrous sodium carbonates at different temperatures. Icarus, 2019, 317, 388-411.	2.5	18
28	67P/Churyumov–Gerasimenko active areas before perihelion identified by GIADA and VIRTIS data fusion. Monthly Notices of the Royal Astronomical Society, 2019, 483, 2165-2176.	4.4	8
29	SIMBIO-SYS Near Earth Commissioning Phase: a step forward toward Mercury. , 2019, , .		1
30	Northwest Africa 6232: Visible–near infrared reflectance spectra variability of an olivine diogenite. Meteoritics and Planetary Science, 2018, 53, 2228-2242.	1.6	8
31	Photometric Modeling and VISâ€IR Albedo Maps of Dione From Cassiniâ€VIMS. Geophysical Research Letters, 2018, 45, 2184-2192.	4.0	7
32	Nature, formation, and distribution of carbonates on Ceres. Science Advances, 2018, 4, e1701645.	10.3	83
33	Variations in the amount of water ice on Ceres' surface suggest a seasonal water cycle. Science Advances, 2018, 4, eaao3757.	10.3	43
34	Laboratory simulations of the Vis-NIR spectra of comet 67P using sub-µm sized cosmochemical analogues. Icarus, 2018, 306, 306-318.	2.5	23
35	Summer outbursts in the coma of comet 67P/Churyumov–Gerasimenko as observed by Rosetta–VIRTIS. Monthly Notices of the Royal Astronomical Society, 2018, 481, 1235-1250.	4.4	20
36	Photometric Modeling and VISâ€IR Albedo Maps of Tethys From Cassiniâ€VIMS. Geophysical Research Letters, 2018, 45, 6400-6407.	4.0	6

#	Article	IF	CITATIONS
37	Localized aliphatic organic material on the surface of Ceres. Science, 2017, 355, 719-722.	12.6	152
38	Evidence for the formation of comet 67P/Churyumov-Gerasimenko through gravitational collapse of a bound clump of pebbles. Monthly Notices of the Royal Astronomical Society, 2017, 469, S755-S773.	4.4	146
39	The pre-launch characterization of SIMBIO-SYS/VIHI imaging spectrometer for the BepiColombo mission to Mercury. I. Linearity, radiometry, and geometry calibrations. Review of Scientific Instruments, 2017, 88, 094502.	1.3	10
40	The pre-launch characterization of SIMBIO-SYS/VIHI imaging spectrometer for the BepiColombo mission to Mercury. II. Spectral calibrations. Review of Scientific Instruments, 2017, 88, 094503.	1.3	8
41	Comet 67P outbursts and quiescent coma at 1.3 au from the Sun: dust properties from Rosetta/VIRTIS-H observations. Monthly Notices of the Royal Astronomical Society, 2017, 469, S443-S458.	4.4	56
42	Rosetta Alice/VIRTIS observations of the water vapour UV electroglow emissions around comet 67P/Churyumov–Gerasimenko. Monthly Notices of the Royal Astronomical Society, 2017, 469, S416-S426.	4.4	12
43	Cometary coma dust size distribution from in situ IR spectra. Monthly Notices of the Royal Astronomical Society, 2017, 469, S598-S605.	4.4	12
44	How pristine is the interior of the comet 67P/Churyumov–Gerasimenko?. Monthly Notices of the Royal Astronomical Society, 2017, 469, S685-S694.	4.4	22
45	Photometric behaviour of 67P/Churyumov–Gerasimenko and analysis of its pre-perihelion diurnal variations. Monthly Notices of the Royal Astronomical Society, 2017, 469, S346-S356.	4.4	16
46	Three-dimensional direct simulation Monte-Carlo modeling of the coma of comet 67P/Churyumov-Gerasimenko observed by the VIRTIS and ROSINA instruments on board Rosetta. Astronomy and Astrophysics, 2016, 588, A134.	5.1	88
47	Detection of exposed H ₂ O ice on the nucleus of comet 67P/Churyumov-Gerasimenko. Astronomy and Astrophysics, 2016, 595, A102.	5.1	67
48	Water and carbon dioxide distribution in the 67P/Churyumov-Gerasimenko coma from VIRTIS-M infrared observations. Astronomy and Astrophysics, 2016, 589, A45.	5.1	62
49	Visible and Near-Infrared (VNIR) reflectance spectroscopy of glassy igneous material: Spectral variation, retrieving optical constants and particle sizes by Hapke model. Icarus, 2016, 266, 267-278.	2.5	15
50	Investigation into the disparate origin of CO2 and H2O outgassing for Comet 67/P. Icarus, 2016, 277, 78-97.	2.5	61
51	Refractory and semi-volatile organics at the surface of comet 67P/Churyumov-Gerasimenko: Insights from the VIRTIS/Rosetta imaging spectrometer. Icarus, 2016, 272, 32-47.	2.5	127
52	The global surface composition of 67P/CG nucleus by Rosetta/VIRTIS. (I) Prelanding mission phase. Icarus, 2016, 274, 334-349.	2.5	54
53	Cassini's geological and compositional view of Tethys. Icarus, 2016, 274, 1-22.	2.5	13
54	Direct Simulation Monte Carlo modelling of the major species in the coma of comet 67P/Churyumov-Gerasimenko. Monthly Notices of the Royal Astronomical Society, 2016, 462, S156-S169.	4.4	87

#	Article	IF	CITATIONS
55	Evolution of CO ₂ , CH ₄ , and OCS abundances relative to H ₂ O in the coma of comet 67P around perihelion from <i>Rosetta</i> /VIRTIS-H observations. Monthly Notices of the Royal Astronomical Society, 2016, 462, S170-S183.	4.4	72
56	Distribution of phyllosilicates on the surface of Ceres. Science, 2016, 353, .	12.6	159
57	Seasonal exposure of carbon dioxide ice on the nucleus of comet 67P/Churyumov-Gerasimenko. Science, 2016, 354, 1563-1566.	12.6	61
58	Disk-resolved photometry of Vesta and Lutetia and comparison with other asteroids. Icarus, 2016, 267, 204-216.	2.5	11
59	Saturn's icy satellites investigated by Cassini-VIMS. IV. Daytime temperature maps. Icarus, 2016, 271, 292-313.	2.5	23
60	Bright carbonate deposits as evidence of aqueous alteration on (1) Ceres. Nature, 2016, 536, 54-57.	27.8	240
61	Exposed water ice on the nucleus of comet 67P/Churyumov–Gerasimenko. Nature, 2016, 529, 368-372.	27.8	104
62	First observations of H ₂ O and CO ₂ vapor in comet 67P/Churyumov-Gerasimenko made by VIRTIS onboard Rosetta. Astronomy and Astrophysics, 2015, 583, A6.	5.1	77
63	Photometric properties of comet 67P/Churyumov-Gerasimenko from VIRTIS-M onboard Rosetta. Astronomy and Astrophysics, 2015, 583, A31.	5.1	71
64	Terrestrial <scp>OH</scp> nightglow measurements during the <scp>Rosetta</scp> flyby. Geophysical Research Letters, 2015, 42, 5670-5677.	4.0	7
65	Ammoniated phyllosilicates with a likely outer Solar System origin on (1) Ceres. Nature, 2015, 528, 241-244.	27.8	276
66	The organic-rich surface of comet 67P/Churyumov-Gerasimenko as seen by VIRTIS/Rosetta. Science, 2015, 347, aaa0628.	12.6	293
67	Mineralogical and spectral analysis of Vesta's Gegania and Lucaria quadrangles and comparative analysis of their key features. Icarus, 2015, 259, 72-90.	2.5	19
68	The diurnal cycle of water ice on comet 67P/Churyumov–Gerasimenko. Nature, 2015, 525, 500-503.	27.8	199
69	VIRTIS on Rosetta: a unique technique to observe comet 67P/Churyumov-Gerasimenko – first results and prospects. Proceedings of SPIE, 2015, , .	0.8	4
70	Detections and geologic context of local enrichments in olivine on Vesta with VIR/Dawn data. Journal of Geophysical Research E: Planets, 2014, 119, 2078-2108.	3.6	33
71	Characterization of the integrating sphere for the on-ground calibration of the SIMBIOSYS instrument for the BepiColombo ESA mission. Proceedings of SPIE, 2014, , .	0.8	6
72	Composition and mineralogy of dark material units on Vesta. Icarus, 2014, 240, 58-72.	2.5	41

#	Article	IF	CITATIONS
73	Thermal measurements of dark and bright surface features on Vesta as derived from Dawn/VIR. Icarus, 2014, 240, 36-57.	2.5	52
74	Spectroscopic classification of icy satellites of Saturn II: Identification of terrain units on Rhea. Icarus, 2014, 234, 1-16.	2.5	26
75	A test of Hapke's model by means of Monte Carlo ray-tracing. Icarus, 2014, 237, 293-305.	2.5	22
76	Cassini–VIMS observations of Saturn's main rings: I. Spectral properties and temperature radial profiles variability with phase angle and elevation. Icarus, 2014, 241, 45-65.	2.5	24
77	Analysis of Rosetta/VIRTIS spectra of earth using observations from ENVISAT/AATSR, TERRA/MODIS and ENVISAT/SCIAMACHY, and radiative-transfer simulations. Planetary and Space Science, 2014, 90, 37-59.	1.7	6
78	Spectral variability of plagioclase–mafic mixtures (2): Investigation of the optical constant and retrieved mineral abundance dependence on particle size distribution. Icarus, 2014, 235, 207-219.	2.5	30
79	Photometric behavior of spectral parameters in Vesta dark and bright regions as inferred by the Dawn VIR spectrometer. Icarus, 2014, 240, 20-35.	2.5	51
80	Spectral analysis of the bright materials on the asteroid Vesta. Icarus, 2014, 240, 73-85.	2.5	26
81	Compositional evidence of magmatic activity on Vesta. Geophysical Research Letters, 2014, 41, 3038-3044.	4.0	12
82	Spectroscopic classification of icy satellites of saturn — Identification of terrain units on dione and rhea. , 2014, , .		0
83	Vesta surface thermal properties map. Geophysical Research Letters, 2014, 41, 1438-1443.	4.0	46
84	Connections between spectra and structure in Saturn's main rings based on Cassini VIMS data. Icarus, 2013, 223, 105-130.	2.5	40
85	Olivine thermal emissivity under extreme temperature ranges: Implication for Mercury surface. Earth and Planetary Science Letters, 2013, 371-372, 252-257.	4.4	20
86	Pre-launch calibrations of the Vis-IR Hyperspectral Imager (VIHI) onboard BepiColombo, the ESA mission to Mercury. Proceedings of SPIE, 2013, , .	0.8	5
87	Spectral variability of plagioclase–mafic mixtures (1): Effects of chemistry and modal abundance in reflectance spectra of rocks and mineral mixtures. Icarus, 2013, 226, 282-298.	2.5	52
88	Spectroscopic classification of icy satellites of Saturn I: Identification of terrain units on Dione. Icarus, 2013, 226, 1331-1349.	2.5	22
89	Comparative analysis of airglow emissions in terrestrial planets, observed with VIRTIS-M instruments on board Rosetta and Venus Express. Icarus, 2013, 226, 1115-1127.	2.5	11
90	THE RADIAL DISTRIBUTION OF WATER ICE AND CHROMOPHORES ACROSS SATURN'S SYSTEM. Astrophysical Journal, 2013, 766, 76.	4.5	26

#	Article	IF	CITATIONS
91	Vestan lithologies mapped by the visual and infrared spectrometer on Dawn. Meteoritics and Planetary Science, 2013, 48, 2185-2198.	1.6	75
92	The heating history of Vesta and the onset of differentiation. Meteoritics and Planetary Science, 2013, 48, 2316-2332.	1.6	27
93	Vesta's mineralogical composition as revealed by the visible and infrared spectrometer on Dawn. Meteoritics and Planetary Science, 2013, 48, 2166-2184.	1.6	87
94	Olivine in an unexpected location on Vesta's surface. Nature, 2013, 504, 122-125.	27.8	82
95	THE ONSET OF DIFFERENTIATION AND INTERNAL EVOLUTION: THE CASE OF 21 LUTETIA. Astrophysical Journal, 2013, 770, 50.	4.5	1
96	Composition of the Rheasilvia basin, a window into Vesta's interior. Journal of Geophysical Research E: Planets, 2013, 118, 335-346.	3.6	84
97	Thermal analysis of unusual local-scale features on the surface of Vesta. , 2013, , .		0
98	Photometric Properties of Vesta. Proceedings of the International Astronomical Union, 2012, 10, 179-179.	0.0	2
99	The visible and near infrared (VNIR) spectrometer of EChO. , 2012, , .		2
100	Dark material on Vesta from the infall of carbonaceous volatile-rich material. Nature, 2012, 491, 83-86.	27.8	151
101	Pitted Terrain on Vesta and Implications for the Presence of Volatiles. Science, 2012, 338, 246-249.	12.6	91
102	Saturn's icy satellites and rings investigated by Cassini–VIMS: III – Radial compositional variability. Icarus, 2012, 220, 1064-1096.	2.5	86
103	Interpretation of combined infrared, submillimeter, and millimeter thermal flux data obtained during the Rosetta fly-by of Asteroid (21) Lutetia. Icarus, 2012, 221, 395-404.	2.5	47
104	DETECTION OF WIDESPREAD HYDRATED MATERIALS ON VESTA BY THE VIR IMAGING SPECTROMETER ON BOARD THE <i>DAWN</i> MISSION. Astrophysical Journal Letters, 2012, 758, L36.	8.3	117
105	Spectroscopic Characterization of Mineralogy and Its Diversity Across Vesta. Science, 2012, 336, 697-700.	12.6	240
106	Mapping Titan's surface features within the visible spectrum via Cassini VIMS. Planetary and Space Science, 2012, 60, 52-61.	1.7	25
107	Overview of Lutetia's surface composition. Planetary and Space Science, 2012, 66, 23-30.	1.7	29
108	The light curve of asteroid 21 Lutetia measured by VIRTIS-M during the Rosetta fly-by. Planetary and Space Science, 2012, 66, 9-22.	1.7	12

#	Article	IF	CITATIONS
109	Thermal properties of the asteroid (2867) Steins as observed by VIRTIS/Rosetta. Astronomy and Astrophysics, 2011, 531, A168.	5.1	29
110	Hapke modeling of Rhea surface properties through Cassini-VIMS spectra. Icarus, 2011, 214, 541-555.	2.5	64
111	The Surface Composition and Temperature of Asteroid 21 Lutetia As Observed by Rosetta/VIRTIS. Science, 2011, 334, 492-494.	12.6	110
112	Correlations between VIMS and RADAR data over the surface of Titan: Implications for Titan's surface properties. Icarus, 2010, 208, 366-384.	2.5	8
113	SIMBIO-SYS: The spectrometer and imagers integrated observatory system for the BepiColombo planetary orbiter. Planetary and Space Science, 2010, 58, 125-143.	1.7	70
114	VIS-NIR Imaging Spectroscopy of Mercury's Surface: SIMBIO-SYS/VIHI Experiment Onboard the BepiColombo Mission. IEEE Transactions on Geoscience and Remote Sensing, 2010, , .	6.3	14
115	The light curve of asteroid 2867 Steins measured by VIRTIS-M during the Rosetta fly-by. Planetary and Space Science, 2010, 58, 1066-1076.	1.7	11
116	Saturn's icy satellites investigated by Cassini–VIMS. Icarus, 2010, 206, 507-523.	2.5	47
117	Martian atmosphere as observed by VIRTISâ€M on Rosetta spacecraft. Journal of Geophysical Research, 2010, 115, .	3.3	10
118	VIS-NIR imaging spectroscopy of the Mercury's surface: SIMBIO-SYS/VIHI experiment onboard the Bepi Colombo mission. , 2009, , .		0
119	Visible and near infrared detector for BepiColombos spectrometer VIHI. EAS Publications Series, 2009, 37, 391-395.	0.3	2
120	VIMS spectral mapping observations of Titan during the Cassini prime mission. Planetary and Space Science, 2009, 57, 1950-1962.	1.7	28
121	Saturn's Titan: Surface change, ammonia, and implications for atmospheric and tectonic activity. Icarus, 2009, 199, 429-441.	2.5	69
122	Saturn Satellites as Seen by Cassini Mission. Earth, Moon and Planets, 2009, 105, 289-310.	0.6	4
123	Triple F—a comet nucleus sample return mission. Experimental Astronomy, 2009, 23, 809-847.	3.7	14
124	Calibration pipeline of VIS-NIR imaging spectrometers for planetary exploration: The rosetta VIRTIS-M case. , 2009, , .		3
125	Photometric changes on Saturn's Titan: Evidence for active cryovolcanism. Geophysical Research Letters, 2009, 36, .	4.0	38
126	VIRTIS: An Imaging Spectrometer for the ROSETTA Mission. , 2009, , 563-585.		3

8

#	Article	IF	CITATIONS
127	Hydrocarbons on Saturn's satellites lapetus and Phoebe. Icarus, 2008, 193, 334-343.	2.5	86
128	Identification of spectral units on Phoebe. Icarus, 2008, 193, 233-251.	2.5	32
129	A close look at Saturn's rings with Cassini VIMS. Icarus, 2008, 193, 182-212.	2.5	113
130	Saturn's icy satellites investigated by Cassini-VIMS. Icarus, 2007, 186, 259-290.	2.5	62
131	BepiColombo SIMBIO-SYS data: Preliminary evaluation for rock discrimination and recognition in both low and high resolution spectroscopic data in the visible and near infrared spectral intervals. Planetary and Space Science, 2007, 55, 1596-1613.	1.7	9
132	Surface composition of Hyperion. Nature, 2007, 448, 54-56.	27.8	56
133	A dynamic upper atmosphere of Venus as revealed by VIRTIS on Venus Express. Nature, 2007, 450, 641-645.	27.8	95
134	South-polar features on Venus similar to those near the north pole. Nature, 2007, 450, 637-640.	27.8	110
135	Dawn Mission to Vesta and Ceres. Earth, Moon and Planets, 2007, 101, 65-91.	0.6	125
136	Virtis: An Imaging Spectrometer for the Rosetta Mission. Space Science Reviews, 2007, 128, 529-559.	8.1	181
137	Observations in the Saturn system during approach and orbital insertion, with Cassini's visual and infrared mapping spectrometer (VIMS). Astronomy and Astrophysics, 2006, 446, 707-716.	5.1	57
138	High-resolution CASSINI-VIMS mosaics of Titan and the icy Saturnian satellites. Planetary and Space Science, 2006, 54, 1146-1155.	1.7	24
139	Photometric properties of Titan's surface from Cassini VIMS: Relevance to titan's hemispherical albedo dichotomy and surface stability. Planetary and Space Science, 2006, 54, 1540-1551.	1.7	13
140	Global Mineralogical and Aqueous Mars History Derived from OMEGA/Mars Express Data. Science, 2006, 312, 400-404.	12.6	1,395
141	THE ATMOSPHERES OF SATURN AND TITAN IN THE NEAR-INFRARED: FIRST RESULTS OF CASSINI/VIMS. Earth, Moon and Planets, 2006, 96, 119-147.	0.6	57
142	G-MODE CLASSIFICATION OF SPECTROSCOPIC DATA. Earth, Moon and Planets, 2006, 96, 165-197.	0.6	8
143	Dawn Discovery mission to Vesta and Ceres: Present status. Advances in Space Research, 2006, 38, 2043-2048.	2.6	26
144	Composition and Physical Properties of Enceladus' Surface. Science, 2006, 311, 1425-1428.	12.6	199

#	Article	IF	CITATIONS
145	On-ground characterization of Rosetta/VIRTIS-M. II. Spatial and radiometric calibrations. Review of Scientific Instruments, 2006, 77, 103106.	1.3	34
146	On-ground characterization of Rosetta/VIRTIS-M. I. Spectral and geometrical calibrations. Review of Scientific Instruments, 2006, 77, 093109.	1.3	42
147	Cassini Visual and Infrared Mapping Spectrometer Observations of Iapetus: Detection of CO 2. Astrophysical Journal, 2005, 622, L149-L152.	4.5	94
148	A 5-Micron-Bright Spot on Titan: Evidence for Surface Diversity. Science, 2005, 310, 92-95.	12.6	78
149	Compositional maps of Saturn's moon Phoebe from imaging spectroscopy. Nature, 2005, 435, 66-69.	27.8	155
150	Release of volatiles from a possible cryovolcano from near-infrared imaging of Titan. Nature, 2005, 435, 786-789.	27.8	208
151	Phyllosilicates on Mars and implications for early martian climate. Nature, 2005, 438, 623-627.	27.8	825
152	Mars Surface Diversity as Revealed by the OMEGA/Mars Express Observations. Science, 2005, 307, 1576-1581.	12.6	842
153	The Evolution of Titan's Mid-Latitude Clouds. Science, 2005, 310, 474-477.	12.6	139
154	METHIS: Mercury thermal infrared spectrometer. Advances in Space Research, 2004, 33, 2189-2194.	2.6	0
155	The Cassini Visual And Infrared Mapping Spectrometer (Vims) Investigation. Space Science Reviews, 2004, 115, 111-168.	8.1	369
156	MEMORIS: a wide angle camera for the BepiColombo mission. Advances in Space Research, 2004, 33, 2182-2188.	2.6	3
157	VISPO project: visible image-spectrometer for planetary observations. New Astronomy, 2004, 9, 635-640.	1.8	0
158	Cassini VIMS observations of the Galilean satellites including the VIMS calibration procedure. Icarus, 2004, 172, 104-126.	2.5	61
159	CASSINI/VIMS-V at Jupiter: Radiometric calibration test and data results. Planetary and Space Science, 2004, 52, 661-670.	1.7	27
160	Principal components analysis of Jupiter VIMS spectra. Advances in Space Research, 2004, 34, 1640-1646.	2.6	4
161	The Cassini Visual and Infrared Mapping Spectrometer (VIMS) Investigation. , 2004, , 111-168.		6
162	Virtis Experiment at Churyumov — Gerasimenko Comet, New Rosetta Target. Astrophysics and Space Science Library, 2004, , 223-236.	2.7	4

#	Article	IF	CITATIONS
163	Observations with the Visual and Infrared Mapping Spectrometer (VIMS) during Cassini's flyby of Jupiter. Icarus, 2003, 164, 461-470.	2.5	48
164	Cassini-VIMS at Jupiter: solar occultation measurements using lo. lcarus, 2003, 166, 75-84.	2.5	7
165	Virtis-H: an infrared spectrometer for the Rosetta mission calibration results. , 2002, 4818, 14.		2
166	Cassini/VIMS observations of the moon. Advances in Space Research, 2002, 30, 1889-1894.	2.6	0
167	Infrared space interferometry $\hat{a} \in \hat{~}$ the DARWIN mission. Advances in Space Research, 2002, 30, 2135-2145.	2.6	24
168	MARS-IRMA: in-situ infrared microscope analysis of Martian soil and rock samples Advances in Space Research, 2001, 28, 1219-1224.	2.6	5
169	The international package for scientific experiments (IPSE) for Mars surveyor program. Advances in Space Research, 2001, 28, 1209-1218.	2.6	Ο
170	MA_MISS: Mars multispectral imager for subsurface studies. Advances in Space Research, 2001, 28, 1203-1208.	2.6	16
171	<title>VIRTIS-H: a high-spectral-resolution channel for the Rosetta infrared imaging spectrometer</title> . , 2000, , .		5
172	Detection of Sub-Micron Radiation from the Surface of Venus by Cassini/VIMS. Icarus, 2000, 148, 307-311.	2.5	62
173	Efficiency measurements of the VIRTIS-M grating. Planetary and Space Science, 2000, 48, 411-417.	1.7	7
174	Numerically improved thermochemical evolution models of comet nuclei. Planetary and Space Science, 1999, 47, 839-853.	1.7	19
175	Models of P/Wirtanen nucleus: active regions versus non-active regions. Planetary and Space Science, 1999, 47, 855-872.	1.7	36
176	VIRTIS: The imaging spectrometer of the Rosetta mission. Advances in Space Research, 1999, 24, 1095-1104.	2.6	22
177	Virtis : an imaging spectrometer for the rosetta mission. Planetary and Space Science, 1998, 46, 1291-1304.	1.7	72
178	An imaging spectrometer operating in the visible near infrared for the study of planetary surfaces. Planetary and Space Science, 1998, 46, 1277-1290.	1.7	2
179	Imaging spectroscopy of Saturn and its satellites : vims-v onboard Cassini. Planetary and Space Science, 1998, 46, 1263-1276.	1.7	11
180	PFS: A fourier spectrometer for the study of Martian atmosphere. Advances in Space Research, 1997, 19, 1277-1280.	2.6	28

#	Article	IF	CITATIONS
181	Transition Elements between Comets and Asteroids. Icarus, 1997, 129, 317-336.	2.5	43
182	Transition Elements between Comets and Asteroids. Icarus, 1997, 129, 337-347.	2.5	38
183	<title>VIRTIS: Visible Infrared Thermal Imaging Spectrometer for the Rosetta mission</title> . , 1996, , .		17
184	Infrared spectrometer PFS for the Mars 94 orbiter. Advances in Space Research, 1996, 17, 61-64.	2.6	15
185	A P/Wirtanen evolution model. Planetary and Space Science, 1996, 44, 987-1000.	1.7	41
186	Thermal evolution and differentiation of a short-period comet. Planetary and Space Science, 1993, 41, 409-427.	1.7	33
187	Planetary Fourier spectrometer: An interferometer for atmospheric studies on board Mars 94 mission. Il Nuovo Cimento Della Società Italiana Di Fisica C, 1993, 16, 575-588.	0.2	4
188	An imaging spectrometer for planetary studies. Il Nuovo Cimento Della Società Italiana Di Fisica C, 1993, 16, 589-595.	0.2	1
189	Phase curves of meteorites and terrestrial rocks: Laboratory measurements and applications to asteroids. Icarus, 1990, 83, 325-348.	2.5	40
190	Asteroidal catastrophic collisions simulated by hypervelocity impact experiments. Icarus, 1986, 66, 487-514.	2.5	51
191	Experimental measurement of particle deceleration and survival in multiple thin foil targets. Advances in Space Research, 1986, 6, 17-20.	2.6	2
192	Radiofrequency emissions observed during macroscopic hypervelocity impact experiments. Nature, 1984, 308, 830-832.	27.8	38
193	Shapes of asteroids compared with fragments from hypervelocity impact experiments. Nature, 1984, 308, 832-834.	27.8	68
194	The temporal evolution of exposed water ice-rich areas on the surface of 67P/Churyumov-Gerasimenko: spectral analysis. Monthly Notices of the Royal Astronomical Society, 0, , stw3281.	4.4	13
195	and seasonal variability. Monthly Notices of the Royal Astronomical Society, 0, , stw3177.	4.4	10
196	GAUSS - genesis of asteroids and evolution of the solar system. Experimental Astronomy, 0, , 1.	3.7	5
197	IPSE: Italian package for scientific experiments. , 0, , .		Ο